The Journal of Nutrition
Nutrient Physiology, Metabolism, and Nutrient-Nutrient Interactions

Intestinal Barrier Function and the Gut Microbiome Are Differentially Affected in Mice Fed a Western-Style Diet or Drinking Water Supplemented with Fructose[1–3]

Valentina Volynets,[4] Sandrine Louis,[4] Dominik Pretz,[4] Lisa Lang,[4] Maureen J Ostaff,[5,6] Jan Wehkamp,[6] and Stephan C Bischoff[4]*

[4]Department of Nutritional Medicine, University of Hohenheim, Stuttgart, Germany; [5]University of Colorado Anschutz Medical Campus, Denver, CO; and [6]Department of Internal Medicine, University of Tübingen, Tübingen, Germany

Abstract

Background: The consumption of a Western-style diet (WSD) and high fructose intake are risk factors for metabolic diseases. The underlying mechanisms are largely unclear.

Objective: To unravel the mechanisms by which a WSD and fructose promote metabolic disease, we investigated their effects on the gut microbiome and barrier function.

Methods: Adult female C57BL/6J mice were fed a sugar- and fat-rich WSD or control diet (CD) for 12 wk and given access to tap water or fructose-supplemented water. The microbiota was analyzed with the use of 16S rRNA gene sequencing. Barrier function was studied with the use of permeability tests, and endotoxin, mucus thickness, and gene expressions were measured.

Results: The WSD increased body weight gain but not endotoxin translocation compared with the CD. In contrast, high fructose intake increased endotoxin translocation 2.6- and 3.8-fold in the groups fed the CD + fructose and WSD + fructose, respectively, compared with the CD group. The WSD + fructose treatment also induced a loss of mucus thickness in the colon (−46%) and reduced defensin expression in the ileum and colon. The lactulose:mannitol ratio in the WSD + fructose mice was 1.8-fold higher than in the CD mice. Microbiota analysis revealed that fructose, but not the WSD, increased the Firmicutes:Bacteroidetes ratio by 88% for CD + fructose and 63% for WSD + fructose compared with the CD group. *Bifidobacterium* abundance was greater in the WSD mice than in the CD mice (63-fold) and in the WSD + fructose mice than in the CD + fructose mice (330-fold).

Conclusions: The consumption of a WSD or high fructose intake differentially affects gut permeability and the microbiome. Whether these differences are related to the distinct clinical outcomes, whereby the WSD primarily promotes weight gain and high fructose intake causes barrier dysfunction, needs to be investigated in future studies. *J Nutr* 2017;147:770–80.

Keywords: defensin, Western-style diet, fructose, gut microbiome, permeability

Introduction

Overfeeding, either globally or with respect to particular nutrients, is common throughout the world and recognized as a risk factor for cardiovascular, metabolic, and malignant diseases (1–3). Both increased energy intake and the high intake of nutrients, such as fat and sugar, contribute to the risk of developing such diseases. Preclinical experiments have revealed that an energy-dense high-fat and high-sugar diet, also called a Western-style diet (WSD)[7], causes insulin resistance, cancer, and impaired stimulus control (4–6). Such data strongly suggest that a WSD, which is common and relevant among other factors in regard to overfeeding, contributes to the major disease burdens of industrialized and developing countries. However,

[1] Supported by German Research Foundation grant BI 424/8-1 and Federal Ministry of Education and Research grant 01GI1122H (both to SCB).
[2] Author disclosures: V Volynets, S Louis, D Pretz, L Lang, MJ Ostaff, J Wehkamp, and SC Bischoff, no conflicts of interest.
[3] Supplemental Figure 1 and Supplemental Tables 1–4 are available from the "Online Supporting Material" link in the online posting of the article and from the same link in the online table of contents at http://jn.nutrition.org.
*To whom correspondence should be addressed. E-mail: bischoff.stephan@uni-hohenheim.de.

[7] Abbreviations used: AU, arbitrary unit; CD, control diet; FITC-D4000, fluorescein isothiocyanate–labeled dextran 4000; Muc2, mucin 2; PEG4000, polyethylene glycol 4000; SD-B, standard diet for breeding; *Tff3*, trefoil factor 3; TJ, tight junction; T_0, start of experiment; T_{12}, feeding for 12 wk; WSD, Western-style diet; *ZO-1*, zonula occludens 1.

Manuscript received October 11, 2016. Initial review completed November 15, 2016. Revision accepted February 23, 2017.
First published online March 29, 2017; doi:10.3945/jn.116.242859.

how high loads of fat and sugar promote such diseases is still largely unclear.

Diet is both a short- and long-term major regulator of the intestinal microbiota, which allows for adaptation in terms of food availability and the optimization of energy harvest from food (7–9). On the other hand, this interaction might have negative consequences for weight regulation and susceptibility for disease, as shown for diabetes, cancer, autoimmunity, and frailty in the elderly (10–13). Therefore, the diet-microbiota relation and closely associated intestinal barrier are of major interest in understanding the large number of diet-related diseases.

In mice, a WSD leads to weight gain, steatosis, and insulin resistance (14, 15). It has been shown that, apart from fat, particular sugars such as fructose promote steatosis and insulin resistance. Fructose, in contrast to sucrose and a WSD, induces only marginal weight gain but pronounced liver steatosis, whereas a WSD leads to weight gain with minor liver steatosis (16, 17). These observations suggest different underlying mechanisms induced by fructose and a WSD.

Therefore, we examined the impact of fructose administration, a sugar- and fat-rich WSD, and the combination of both on the gut microbiome composition and intestinal barrier function. With the use of this approach, we wanted to clarify whether the dietetic effects on body and liver weight are related to changes in the gut microbiome or barrier function.

Methods

Animals and treatments. Female C57BL/6J mice were purchased from Janvier Labs and housed in a specific pathogen-free barrier facility with a controlled environment (inverted 12-h daylight cycle) accredited by the Association for Assessment and Accreditation for Laboratory Animal Care International. All procedures were approved by a local animal care and use committee.

For all experiments, female mice of the same age were used to minimize the effects of confounding factors. Mice were fed a standard diet for breeding (SD-B) (adapted to mouse nutritional requirements) (**Table 1**, **Supplemental Tables 1** and **2**). At the start of the experiment (T_0), mice were aged 8 wk and subdivided into 4 intervention groups. Mice were fed either a high-fat and very-high-sugar WSD (TD88137-modified WSD) or a high-sugar control diet (CD) (CD88137-modified CD to TD88137) (ssniff Spezialitäten GmbH) (Table 1, Supplemental Tables 1 and 2) and had free access to either plain tap water or water containing 30% D(−)-fructose (>99.5% purity) (Carl Roth) for 12 wk. The energy density of a 30% fructose solution is 5.09 kJ/g. Accordingly, 4 feeding groups were examined (CD, CD + fructose, WSD, and WSD + fructose) after feeding for 12 wk (T_{12}). Food intake, fluid intake, and body weight were assessed weekly.

For the assessment of the intestinal barrier, each feeding group was divided into 2 subgroups of 8–9 mice each. After the 12-wk diet phase in subgroup I, 2 intestinal barrier tests [polyethylene glycol 4000 (PEG4000) and lactulose mannitol], an endotoxin measurement, and gut tissue analyses were carried out; in subgroup II, another barrier test [fluorescein isothiocyanate–labeled dextran 4000 (FITC-D400)] was performed. All 3 barrier tests required a single administration of test substances per gavage. Before the gavage, mice were housed in metabolic cages for 6 h to ensure a fasting state for all mice and to collect urine. When barrier tests were completed, the mice were anesthetized with an intraperitoneal injection of ketamine:xylazine (100:16 mg body weight/kg). Blood was collected with the use of a portal vein puncture (subgroup I) or cardiocentesis (subgroup II) just before killing. Gut tissue specimens were collected and frozen immediately in liquid nitrogen and then fixed in neutral-buffered formalin or Carnoy's solution.

Immunofluorescence staining of mucin and localization of bacteria by fluorescent in situ hybridization. To analyze bacteria localization at the surface of the intestinal mucosa, intestinal mucin and adjacent bacteria were visualized with the use of mucin 2 (Muc2) immunofluorescence (primary antibody: H-300 sc-15334; Santa Cruz Biotechnology) combined with fluorescent in situ hybridization with the use of the 16S rRNA EUB338 probe (18) (5′-GCTGCCTCCCGTAGGAGT-3′ with a cyanine 3 label; biomers.net GmbH) as previously described (19). For DNA staining, 1 μg 4′,6-diamidino-2-phenylindol dihydrochloride/mL (Carl Roth) was used. The slides were mounted with the use of an antifade mounting medium (Vectashield H-1000; Vector Laboratories). Tissue sections were analyzed with the use of an Axiovert 200M ZEISS fluorescence microscope (Carl Zeiss) at a magnification of 200 times. In colon tissues, adherent mucus-layer thickness (equal the distance of bacteria to the intestinal epithelial cells) was measured perpendicular to the mucosal surface from the edge of the epithelium to the outermost part of the mucus layer and expressed in μm with the use of AxioVision 4.8.2 software. The analysis was based on 10 independent measurements.

RNA isolation and real-time RT-PCR. RNA isolation and real-time RT-PCR were performed as previously described (20) to measure *Muc2*, trefoil factor 3 (*Tff3*), occludin, claudin-2, claudin-5, and zonula

TABLE 1 Nutrient formulation of the standard and experimental diets fed to female mice for 12 wk[1]

	Diet		
	SD-B	CD	WSD
Product	ssniff M-Z Erich, nonpurified	ssniff EF R/M CD88137, purified	ssniff EF R/M TD88137, purified
Diet specification	High protein	High sugar	High sugar, high fat
CP, g/kg	230	171	171
CL, g/kg	60	51	212
Cholesterol, g/kg	—	—	2.071
CF, g/kg	33	50	50
Crude ash, g/kg	68	42	45
Starch, g/kg	344	390	145
Sucrose, g/kg	52	233	328
ME, MJ/kg	14.3	15.7	18.6
CP, kJ/%	36.0	18.0	15.0
CL, kJ/%	15.0	12.0	42.0
Carbohydrates, kJ/%	49.0	70.0	43.0

[1] CD, control diet; CF, crude fiber; CL, crude fat; CP, crude protein; ME, metabolizable energy; SD-B, standard high-energy diet for breeding; WSD, Western-style diet.

TABLE 2 Energy intake, body and liver weight, plasma TG concentrations, and intestinal barrier markers in blood and urine in female mice fed a CD or WSD with or without 30% fructose for 12 wk[1]

	Diet groups[2]				*P*		
Parameters	CD	CD + F	WSD	WSD + F	DxF	D	F
Food intake per mouse, g/d	2.81 ± 0.1[a]	1.60 ± 0.03[c]	2.89 ± 0.1[a]	2.18 ± 0.1[b]	<0.05	<0.05	<0.01
Energy from diet, kJ/d	43.6 ± 1.2[b]	24.7 ± 0.4[c]	55.1 ± 2.0[a]	41.7 ± 1.8[b]	NS	<0.01	NS
Energy from fructose, kJ/d	—	26.2 ± 0.4	—	19.7 ± 0.6*			
Total energy intake, kJ/d	43.4 ± 1.3[c]	50.9 ± 0.5[b,c]	55.1 ± 2.0[a,b]	61.4 ± 1.2[a]	NS	<0.01	<0.01
Body weight gain, g/12wk	3.16 ± 0.2[b]	3.96 ± 0.3[b]	9.97 ± 0.7[a]	8.81 ± 0.5[a]	<0.05	<0.01	NS
Liver weight, g	0.88 ± 0.03[b]	1.21 ± 0.02[a]	1.41 ± 0.1[a]	1.58 ± 0.1[a]	NS	<0.01	<0.01
Liver-to–body weight ratio,%	4.26 ± 0.2[c]	5.42 ± 0.1[a,b]	5.10 ± 0.2[b]	5.82 ± 0.2[a]	NS	<0.01	<0.01
Plasma TGs,[3] mg/dL	24.0 ± 3.4[b]	43.4 ± 6.2[a,b]	49.9 ± 8.6[a,b]	48.8 ± 9.2[a]	NS	<0.05	NS
Plasma iFABP-2,[3] ng/mL	62.8 ± 19[b]	66.0 ± 10[b]	74.0 ± 12[a,b]	167 ± 46[a]	0.07	<0.05	0.06
Urine claudin-3,[3] ng/mL	14.9 ± 2.5[b]	38.9 ± 5.1[a]	50.4 ± 12[a]	27.5 ± 5.2[a,b]	<0.01	NS	NS

[1] Values are means ± SEMs, n = 12–16. Means without a common superscript letter differ, $P < 0.05$. *Different from CD + F, $P < 0.05$ (2-factor ANOVA). CD, control diet; D, diet; DxF, interaction between diet and fructose; F, fructose; iFABP-2; intestinal FA-binding protein 2; WSD, Western-style diet.
[2] See Table 1 for details regarding the experimental diets.
[3] Parameters measured only in mouse subgroup I, n = 6–10.

occludens 1 (*ZO-1*) expression. α-Defensins 1 and 4 and β-defensins 1–4 were quantified with the use of real-time RT-PCR with plasmid standards as previously described (20, 21). The oligonucleotide primer sequences are listed in **Supplemental Table 3**.

Microbiota analysis with the use of 16S rRNA gene sequencing. Fresh feces (1–3 pellets) were collected directly from each mouse before and after dietary intervention, frozen in liquid nitrogen, and stored at −80°C until analysis. Of the 16–18 samples/group and time

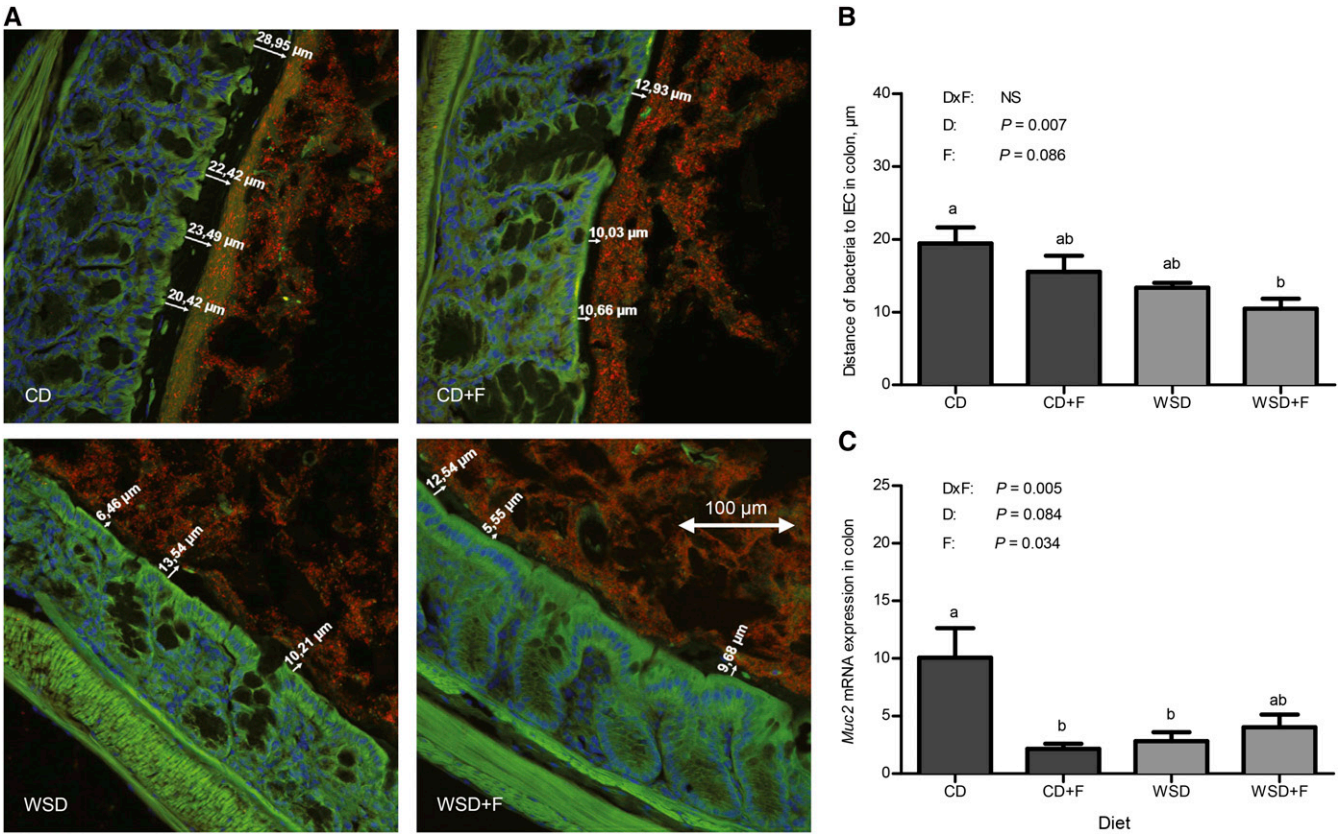

FIGURE 1 Assessment of the mucus thickness (A, B) and *Muc2* mRNA expression (C) in the colon of female mice fed a CD or WSD with or without 30% fructose for 12 wk. (A) Immunofluorescence photomicrographs of the colon specimen stained for Muc2 (green), bacteria (red), and DNA (blue). Representative images are at 200 times magnification. The numbers over the single-headed arrows on the photomicrographs indicate the thickness of the adherent mucus layer (only intact tissue sections were used for this analysis). Double-headed arrow: 100 µm. (B) Mucus thickness (distance of bacteria to IECs) (n = 5–7). (C) *Muc2*-relative mRNA expression normalized to *18S* expression (n = 8–10). Values are means ± SEMs. Means without a common letter differ, $P < 0.05$. CD, control diet; D, diet; DxF, interaction between diet and fructose; F, fructose; IEC, intestinal epithelial cell; Muc2, mucin-2; WSD, Western-style diet.

point, 12 were randomly selected for analysis. After thawing out the samples, metagenomic DNA was extracted with the use of the protocol recommended by the MetaHIT Consortium (22) and quantified before library preparation with the use of fluorometry (Qubit dsDNA HS AssayKit with the use of the Qubit-2.0 fluorometer; Thermo Fisher Scientific). Sequencing analysis and bioinformatics of microbial DNA was performed at the Center for Metagenomics. The libraries were prepared from 12.5 ng metagenomic DNA with the use of the Nextera XT Kit according to the manufacturer's instructions (Illumina Inc.) to analyze the V3-V4 region of the 16S rRNA gene. Sequencing was performed on a HiSeq 2500 (Illumina Inc.) with the use of the rapid mode (2 × 300 bp). Illumina CASAVA version 1.8.2 was used to demultiplex the reads. A quality check was performed with the use of FASTQC version 0.10.1 (Babraham Institute). Quality trimming was performed with the use of Prinseq version 0.20.4 before and after merging with FLASH version 1.2.11 (23, 24). Alignment against the National Center for Biotechnology Information 16S microbial database was carried out with the use of MALT version 0.2.0 (25). Finally, last common ancestor analysis was performed with the use of MEGAN6 (26) as previously described (27). Taxa, the abundance of which was below the detection limit, were given the relative abundance value [in arbitrary units (AUs)] of 0 for further statistical analyses. The 16S sequences are available from the National Center for Biotechnology Information server under BioProject ID PRJNA302359.

Real-time PCR for microbiome analysis. 16S rRNA gene copies (at the metagenome level) were quantified with plasmid standards (from 10^4 to 10^8 for both Bacteroidetes and Firmicutes and from 10^3 to 10^7 for *Bifidobacterium*) with the use of the EvaGreen Universal PCR Master Mix and a CFX96 iCycler (Bio-Rad Laboratories) with an initial hold step (98°C for 2′) and 30 cycles of a 2-step PCR: 95°C for 10′′, annealing temperature for 10′′ (annealing temperature equal to 60°C or 61.5°C for Bacteroidetes or Firmicutes, respectively), and 58°C for 40′′ for *Bifidobacterium*. Primers were taken from the literature [Bacteroidetes (28), Firmicutes (29), and *Bifidobacterium* (30)], tested for specificity against the Silva database (31), and used at a final concentration of 500 nmol/L. The oligonucleotide primer sequences are listed in Supplemental Table 3.

Endotoxin/LPS measurement. LPS was measured in subgroup I, in which portal vein blood was collected, heparinized, and diluted 1:50. Endotoxin concentrations were determined with the use of a limulus amebocyte lysate kinetic assay (LAL Endosafe Endochrome-K, R1710K; Charles River) as previously described (32).

Other urine and plasma measurements. Concentrations of claudin-3 in urine and intestinal FA-binding protein 2 in plasma were determined with the use of high-sensitive ELISA assays (SEF293Mu and SEA559Mu; Hölzl) as described previously (20). Plasma TGs were determined with the use of a commercial kit and quality control level 2 (TR 210 and HN 5067; Randox Laboratories). Colorimetric analyses were carried out with the use of a spectrophotometer (λ = 500 nm and 37°C) (Multi-Detection Microplate Reader, Synergy TM HT; Bio-Tek) and Gen5 version 2.01.

Intestinal barrier analysis with the use of functional tests. The FITC-D4000, PEG4000, and lactulose mannitol tests were performed. The details of all 3 tests, including the methods for detection of the markers by HPLC and the detection limits, have been described previously (32).

Statistical analysis. Normal distribution was tested with the use of the Kolmogorov-Smirnov test. Normally distributed data from multiple groups at baseline were compared with the use of 1-factor ANOVA and Bonferroni's multiple comparison test. To test the potential effects of diet or fructose (and their interaction) at T_{12}, we performed 2-factor ANOVA with a Tukey multiple comparison test. The homogeneity of variances was tested with the use of Bartlett's test, and raw data were

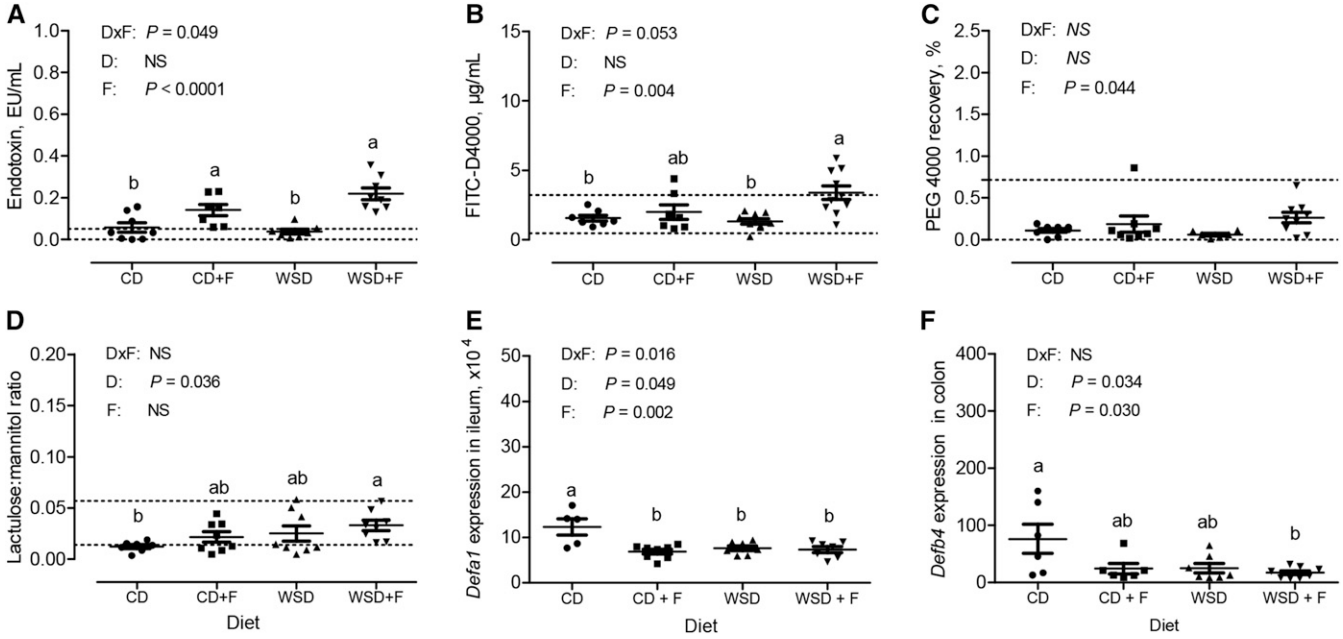

FIGURE 2 Assessment of the intestinal barrier with the use of different markers of permeability (A–D) and defensins (E, F) in female mice fed a CD or WSD with or without 30% fructose for 12 wk. (A) Portal vein blood endotoxin concentration. (B) FITC-D4000 concentration measured in peripheral blood plasma 1 h after gavage. (C) PEG4000 recovery rates measured in urine collected over 24 h after gavage and expressed as percentage of recovery. (D) Lactulose:mannitol ratio calculated from urine recovery rates within 24 h. (E) Mouse *Defa1* mRNA measured in the ileum. (F) Mouse *Defb4* mRNA measured in the colon. Values are means ± SEMs (n = 6–10). Means without a common letter differ, $P < 0.05$. Each point in the graphs represents a single measurement. The dotted horizontal lines indicate lower and upper limits of the normal ranges defined as 90% intervals of data detected in healthy C57BL/6J mice (32). CD, control diet; D, diet; *Defa1*, α-defensin 1; *Defb4*, β-defensin 4; DxF, interaction between diet and fructose; F, fructose; FITC-D4000, fluorescein isothiocyanate–labeled dextran 4000; PEG4000, polyethylene glycol 4000; WSD, Western-style diet.

log-transformed in cases of unequal variances. If only 2 independent groups were compared, either the unpaired *t* test or—if not normally distributed—the Mann-Whitney *U* test was used. For comparisons between the baseline and end of the intervention, we used a paired *t* test or Wilcoxon's test (dependent on normality). Correlation analyses were performed with the use of the Spearman test. $P < 0.05$ was considered statistically significant. The statistical analysis was performed with the use of SPSS version 22 (IBM). For microbiota analysis, the normalized read counts for taxonomic categories were used for all statistical tests with the use of R software (33) and its packages MASS and vegan (34, 35). Nonmetric multidimensional scaling was performed with the use of the Bray-Curtis distance. Benjamini-Hochberg's correction was used for multiple testing. Results are presented as means ± SEMs.

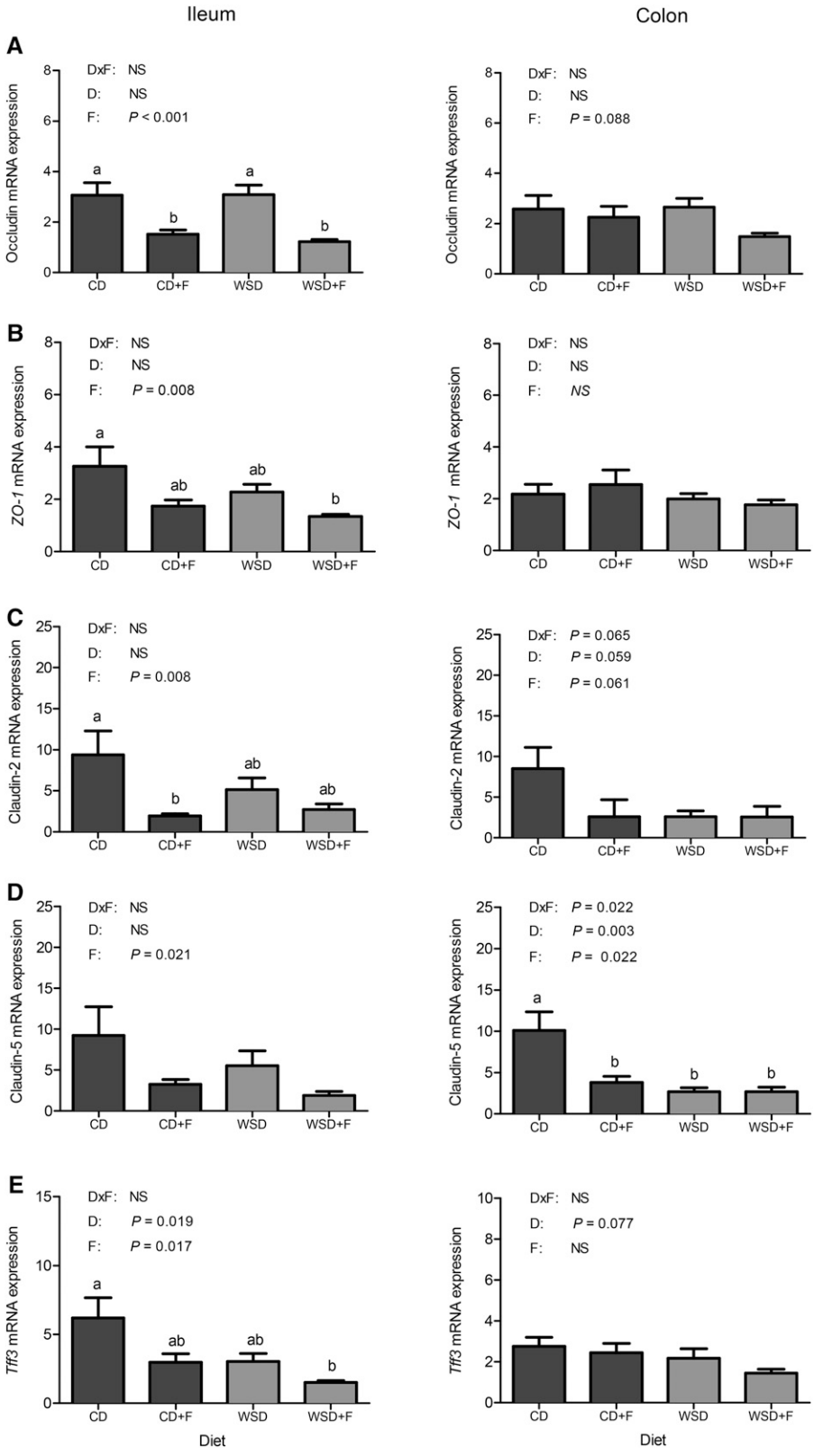

FIGURE 3 Assessment of tight junction (A–D) and *Tff3* (E) mRNA expressions in the ileum and colon of female mice fed a CD or WSD with or without 30% fructose for 12 wk. The mRNA expressions normalized to *18S* expression are shown for (A) occludin, (B) *ZO-1*, (C) claudin-2, (D) claudin-5, and (E) *Tff3* in the ileum (left panels) and colon (right panels). Values are means ± SEMs (n = 6–10). Means without a common letter differ, $P < 0.05$. CD, control diet; D, diet; DxF, interaction between diet and fructose; F, fructose; *Tff3*, trefoil factor 3; WSD, Western-style diet; *ZO-1*, zonula occludens 1.

Results

Diet intake per mouse on the CD or WSD was quite stable (2.8–2.9 g/d) under ad libitum conditions, whereas energy intake was higher after a WSD than those fed the CD. When fructose solution was offered to the mice instead of plain water, diet intake strongly decreased, but total energy intakes did not differ between the CD and CD + fructose groups or between the WSD and WSD + fructose groups (**Table 2**). Consequently, body weight gain over the 12-wk intervention was significantly higher in mice fed the WSD than with the CD (**Supplemental Figure 1**A, Table 2). Body weight gain was closely correlated with the mean energy intake per day ($r = 0.72$; $P < 0.001$) (Supplemental Figure 1B).

Liver weight measured after the intervention correlated with body weight gain (data not shown). Both high fructose intake and a WSD caused an increase in liver weight (38% by fructose and 60% by a WSD compared with a CD) and the liver:body weight ratio (27% by fructose and 20% by a WSD compared with a CD). The combination of both fructose and the WSD also induced a severe increase in liver weight (80%) and in the liver:body weight ratio (37% compared with a CD) (Table 2). Elevated concentrations of plasma TGs and intestinal FA-binding protein 2 were only measured in WSD + fructose–fed mice, whereas fructose intake alone and WSD alone caused elevated concentrations of claudin-3 in urine compared with CD (Table 2).

Fructose intake and a WSD caused several changes in intestinal barrier function. Mucus thickness in the colon was reduced to 10.5 ± 1.3 μm in mice that had received a WSD + fructose compared with 19.4 ± 2.2 μm in CD mice, and *Muc2* mRNA expression was reduced in CD + fructose (2.2 ± 0.4 AUs) and WSD (2.8 ± 0.8 AUs)–fed mice compared with CD mice (10.1 ± 2.6 AUs) (**Figure 1**). Mucus thickness in the colon was negatively correlated with weight gain ($r = -0.47$; $P < 0.01$).

Fructose intake, but not a WSD, resulted in an increase of endotoxin concentration in portal vein blood independent of whether the mice were fed a CD or WSD (**Figure 2**A). LPS concentrations were 2.6-fold higher in mice fed a CD + fructose and 5.7-fold higher in mice fed a WSD + fructose than mice fed a CD or a WSD, respectively ($P < 0.001$ for both). In contrast, the classic intestinal permeability tests (lactulose mannitol and FITC-D4000) consistently revealed increased permeability only

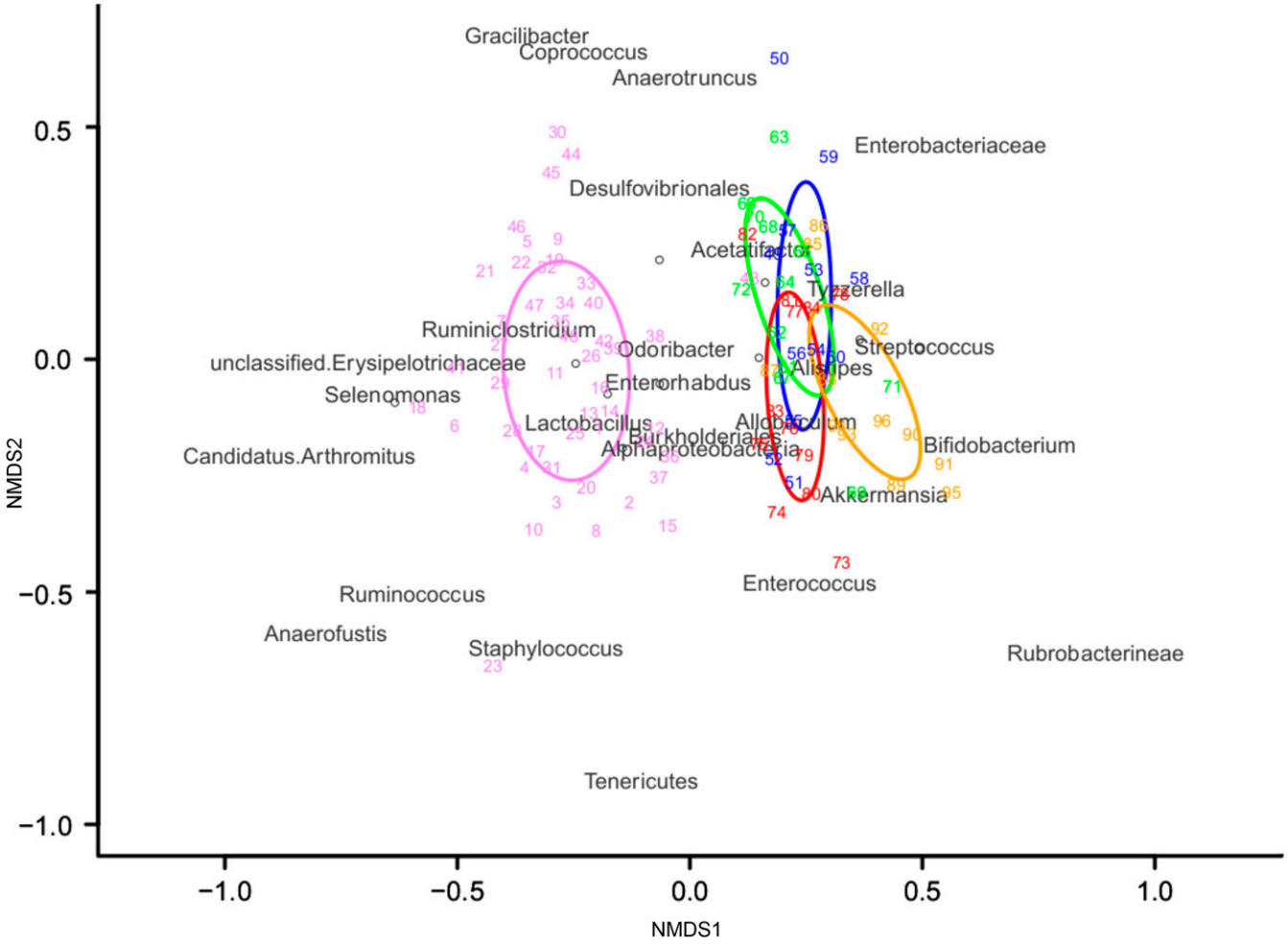

FIGURE 4 NMDS based on the taxonomic composition of all fecal samples of female mice before and after 12 wk of a CD or WSD with or without 30% fructose. This scaling was performed with the use of the Bray-Curtis distance to represent all samples based on their genus-level taxonomic composition (16S rRNA gene sequencing). Individual samples are indicated in arbitrary numbers with the use of different colors. T_0 samples are all colored purple ($n = 48$), and T_{12} samples are colored blue for the CD group, green for the CD + F group, red for the WSD group, and orange for the WSD + F group ($n = 12$ for each T_{12} group). Ellipses represent means ± SDs for each group (with the use of the same color code as for single samples). Bacterial groups are indicated in dark gray letters. CD, control diet; F, fructose; NMDS, nonmetric multidimensional scaling; T_0, start of experiment; T_{12}, feeding for 12 wk; WSD, Western-style diet.

in mice that had received a WSD and fructose simultaneously (Figure 2B, D). For the PEG4000 marker, such an effect was not detected (Figure 2C). In mice fed fructose, a WSD, and the combination thereof, α-defensin 1 mRNA expression in the small intestine was lower than in mice fed a CD (Figure 2E), whereas α-defensin 4 mRNA expression did not change (data not shown). The mRNA of β-defensins 1–4 were analyzed in the colon and showed only a significant difference between the CD and WSD + fructose groups for β-defensins 4 ($P = 0.02$) (Figure 2F). We also measured the mRNA expression of 4 tight junction (TJ) proteins and *Tff3* in the ileum and colon. In the ileum, occludin and claudin-2 mRNA expression levels were lower after fructose administration in mice fed a CD. Occludin, *ZO-1*, and *Tff3* mRNA expression levels were lower after fructose intake in mice fed a WSD. In the colon, only claudin-5 mRNA expression differed after fructose administration compared with the CD group. A WSD compared with a CD did not change any TJ gene expression, except for claudin-5 in the colon (**Figure 3**).

Next, we analyzed the effect of the 4 different dietetic regimens on the fecal microbiota. A mean of 2.07×10^6 reads/sample (range: $0.56–3.56 \times 10^6$) of good quality (Q30 = 76.5%) was yielded from 16S rRNA gene sequencing. As expected, the dominant bacterial phyla were Bacteroidetes and Firmicutes, representing 42% and 47% of the mean community, respectively. The other phyla detected were Proteobacteria (6.5%), Verrucomicrobia (2.8%), and Actinobacteria (1.7%). Members of the phyla Tenericutes could only be detected in one sample.

A nonmetric multidimensional scaling representation of the bacterial genera composition of all samples revealed that each experimental diet (T_{12} data) changed the fecal microbiome compared with the SD-B (T_0) (**Figure 4**). The T_0 data obtained at the beginning of the study when the mice were being fed a standard diet low in fat and sugar were completely separated from all the clusters formed with the T_{12} data. The 4 clusters obtained at T_{12}, when the interventions were completed, were derived from the 4 mouse groups subjected to the 4 different diet regimens. These 4 clusters overlapped. Given the strong effect of switching from the initial SD-B to any of the different experimental diets, which were all high-sugar diets but differed regarding fat content and fructose, we focused on changes in the fecal microbiome between T_0 and T_{12} in more detail. First, we calculated the Shannon diversity index of each sample at the genus level. When comparing samples at T_0 (SD-B) and T_{12} (experimental diets), we found a significantly higher diversity at T_0 (mean: 2.13) than at T_{12} (mean: 1.75; $P < 0.001$). However, no differences in the microbiota diversity could be detected between the 4 different diet groups at T_{12} (data not shown). We could identify several bacterial taxa, the relative abundance of which either increased or decreased when comparing T_0 and T_{12} (**Supplemental Table 4**). Among those that strongly increased were *Parabacteroides* (27-fold), *Alistipes* (8-fold), *Tyzzerella* (10-fold), *Allobaculum* (2-fold), *Acetatifactor* (3-fold), *Bifidobacterium* (20-fold), and *Akkermansia* (4-fold) (all genera). Decreased abundance was found after the intervention for Clostridiales incertae sedis (5-fold; group within the order Clostridiales), unclassified Erysipelotrichaceae (reduced to 0; group within the family Erysipelotrichaceae), and the genera *Ruminiclostridium* (14-fold), *Barnesiella* (3-fold), *Lactobacillus* (4-fold), *Intestinimonas* (41-fold), and *Candidatus arthromitus* (reduced to 0). When these data were analyzed separately for each dietetic group, similar results were obtained for most genera compared with the pooled data analysis. However, *Lactobacillus* was reduced only in mice fed with the CD, whereas *Bifidobacterium* and *Akkermansia* increased only in mice fed the WSD + fructose.

The Firmicutes:Bacteroidetes ratio has been associated with obesity and the metabolic syndrome (10). Therefore, we were interested in the possible effects of the experimental diets on the relative abundance of these 2 phyla. Whereas the abundance of Firmicutes was not affected by the different diets, the abundance of Bacteroidetes was reduced in both groups that received fructose compared with the CD group. These changes in Bacteroidetes abundance resulted in higher Firmicutes:Bacteroidetes ratios in the CD + fructose and WSD + fructose groups than the CD group (**Figure 5**). qPCR confirmed this effect, with significantly lower ratios in the CD group (0.69 ± 0.44) than the CD + fructose (1.38 ± 0.93) and WSD + fructose groups (1.25 ± 0.45) ($P < 0.05$ for both). A strong influence of fructose was revealed ($P < 0.01$; data not shown). Only one other phylum, Verrucomicrobia, was found to be influenced by the

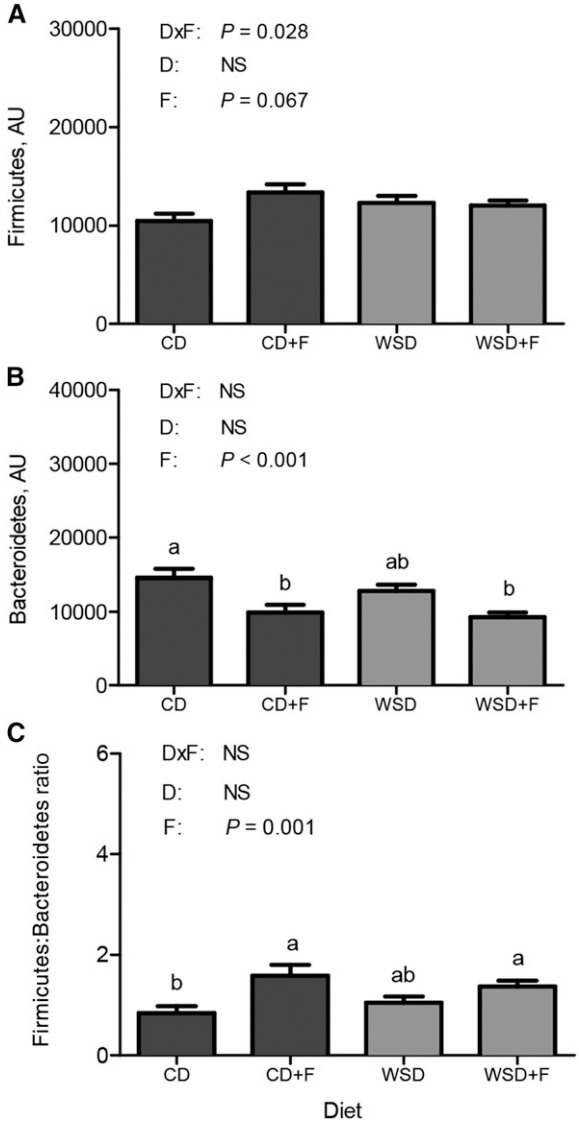

FIGURE 5 Relative abundance of 2 main phyla of the gut microbiota, Firmicutes (A) and Bacteroidetes (B), and their ratio (C) in female mice fed a CD or WSD with or without 30% fructose for 12 wk. Values are means ± SEMs ($n = 12$). Means without a common letter differ, $P < 0.05$. AU, arbitrary unit; CD, control diet; D, diet; F, fructose; DxF, interaction between diet and fructose; WSD, Western-style diet.

intervention, and it tended to be higher in the WSD + fructose group than the other groups ($P = 0.056$; data not shown).

We also found differences between the 4 intervention groups at other taxa levels. The abundance of the genus *Bifidobacterium* was similar in all 4 groups before the intervention (<10 AUs) (**Figure 6**A), but, as mentioned previously, increased after the intervention in the WSD + fructose group (217 ± 44 AUs; $P < 0.001$) (Figure 6B). This strong increase was confirmed by qPCR. Most samples were under the limit of detection, except for the WSD + fructose group (56,153 ± 64,847 16S rRNA gene copies/ng DNA compared with 170 ± 61 for the CD group; data not shown). The relative abundance of the order Burkholderiales was significantly higher in the CD group than the WSD and WSD + fructose groups at T_0 ($P < 0.05$ for both) (Figure 6D), even if all mice were under SD-B. At T_{12}, however, the abundance of Burkholderiales was lower in groups fed CD than in groups fed WSD, revealing a strong effect of diet ($P < 0.001$) (Figure 6E). For the Peptostreptococcaceae family, a strong impact of fructose ($P < 0.01$) was observed, with the relative abundance of this Clostridiales group being lower in the groups that consumed fructose than in the CD group (Figure 6C). For the genus *Parabacteroides*, both diet and fructose showed a strong influence ($P < 0.001$ for both). This genus was much less abundant in the WSD + fructose group than in the CD group ($P < 0.001$) (Figure 6F). The abundance of the order Coriobacteriales was influenced by fructose ($P < 0.001$) and diet ($P < 0.01$). It was significantly higher in the CD + fructose WSD and WSD + fructose groups than in the CD group ($P < 0.05$ for all; data not shown). Finally, the genus *Barnesiella* was significantly reduced in the WSD + fructose group than in the other 3 groups ($P < 0.05$ for all; data not shown). No differences between the 4 groups were found in the abundance of all these taxa at the beginning of the study except for Burkholderiales.

We were also interested in possible correlations between specific taxa and host parameters. When performing Spearman correlation tests, including the T_{12} data from all intervention groups, and correlating all detected bacterial genera abundances with any of the previously reported nonbacterial parameters, we found 4 significant correlations: endotoxin concentrations in portal vein plasma were negatively correlated with Peptostreptococcaceae ($r = -0.60$; $P < 0.01$) (**Figure 7**A) and *Ruminoclostridium* ($r = -0.50$; $P < 0.05$) (Figure 7B) relative abundances; plasma TG concentrations were positively correlated with *Enterorhabdus* ($r = 0.52$; $P < 0.01$) (Figure 7C); and body weight gain after the 12-wk intervention was positively correlated with Burkholderiales ($r = 0.50$; $P < 0.001$) (Figure 7D).

Discussion

Our data confirm that mice challenged with high amounts of fructose develop an impairment of the intestinal barrier, endotoxin translocation to the portal vein, and subsequent liver steatosis (16, 17, 36). We also found that endotoxin translocation in mice fed with a WSD and fructose-rich drinking water is accompanied by a loss of mucus thickness in the colon and a reduced mRNA expression of defensins, *Tff3*, and TJ proteins such as occludin and *ZO-1*. Each TJ protein has its own and different functional properties, some being more extensively studied than others. ZO-1 has been proposed as a master player within the TJ-associated proteins because it binds directly to the cytoplasmic tails of occludin and claudins. Claudins are the main determinants of barrier properties of the TJ. Claudin-2 forms channels for water and small cations, whereas claudin-5 is a "tightening" protein of the paracellular barrier, the absence of which allows molecules <800 Da to pass the barrier (37). Our observed changes in TJ gene expression were associated with increased intestinal permeability in the WSD + fructose–fed mice, as measured by the permeability tests. Moreover, this increase in gut permeability was related to a strong increase in the liver:body weight ratio. This association could explain the link between WSD + fructose consumption and higher liver

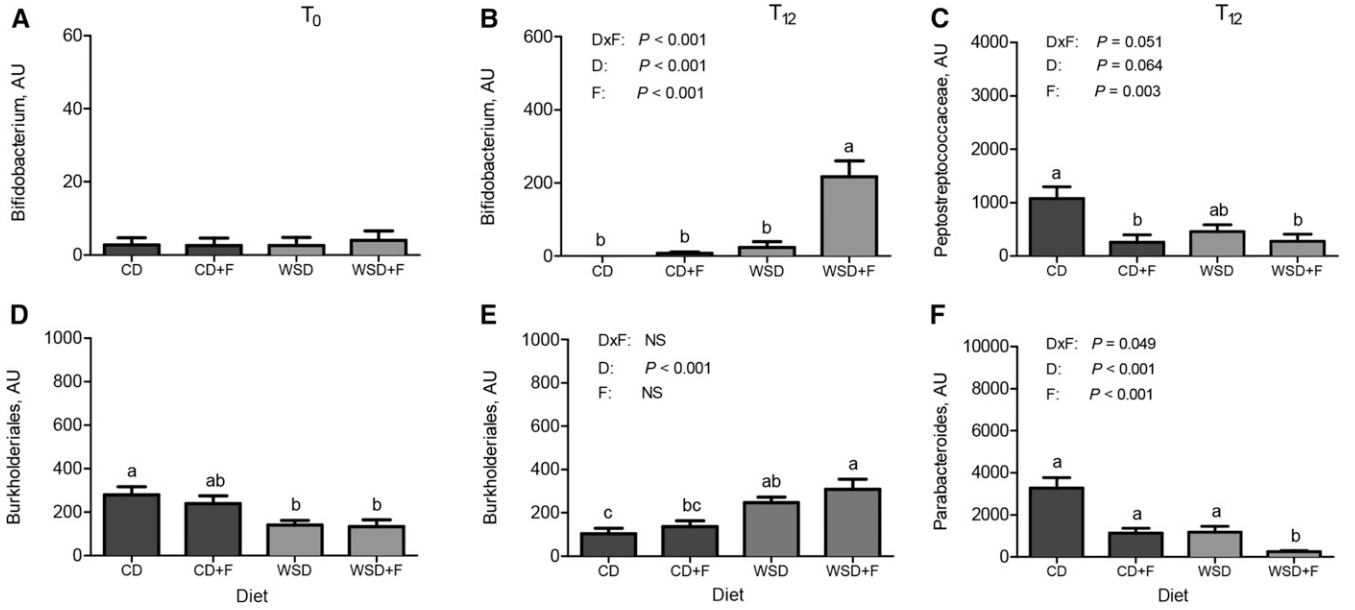

FIGURE 6 Relative abundance of the bacterial genus *Bifidobacterium* (A, B), family Peptostreptococcaceae (C), order Burkholderiales (D, E), and genus *Parabacteroides* (F) in female mice fed a CD or WSD with or without 30% fructose for 12 wk. Gut microbiota 16S rRNA gene analysis was performed at T_0 (A, D) and after T_{12} (B, C, E, F). Values are means ± SEMs ($n = 12$). Means without a common letter differ, $P < 0.05$. AU, arbitrary unit; CD, control diet; D, diet; DxF, interaction between diet and fructose; F, fructose; T_0, start of experiment; T_{12}, feeding for 12 wk; WSD, Western-style diet.

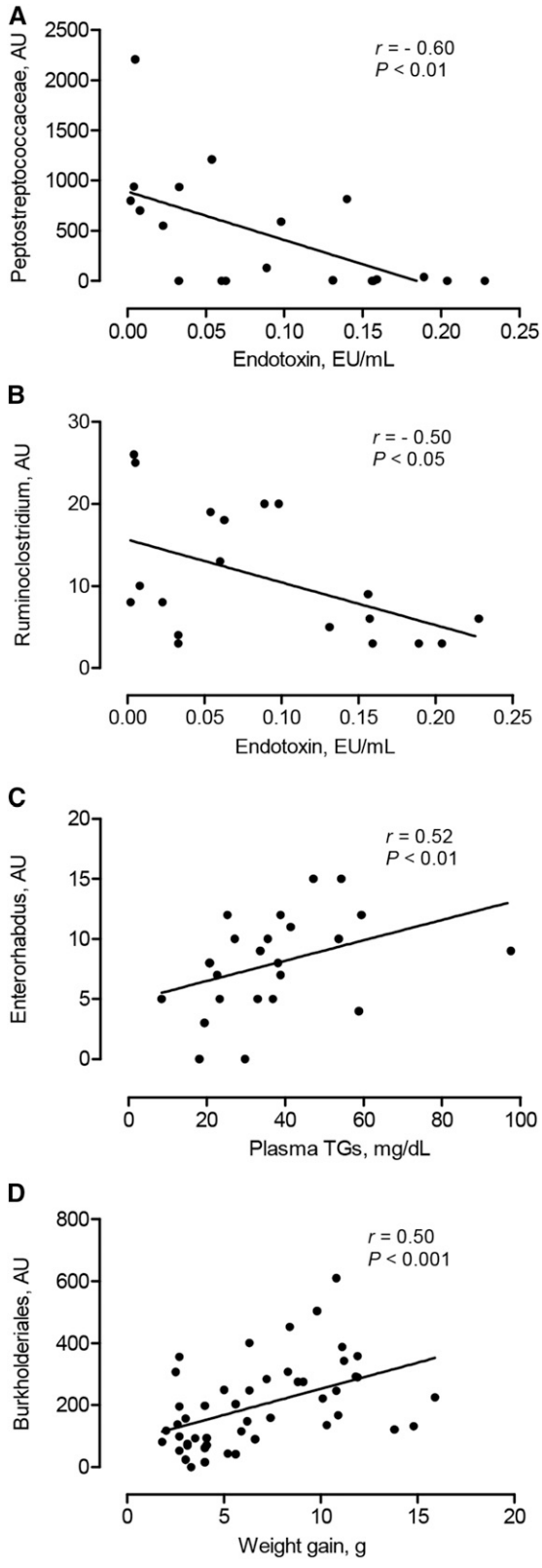

FIGURE 7 Correlations between microbiota taxa abundance and host parameters (A–D) studied in female mice fed a CD or WSD with or without 30% fructose for 12 wk. (A) Portal vein plasma endotoxin concentrations correlated with the relative abundance of the family Peptostreptococcaceae (n = 19) and (B) the genus *Ruminoclostridium* (n = 19). (C) Plasma TGs correlated with the genus *Enterorhabdus* (n = 24). (D) Weight gain over the 12 wk of intervention correlated with the relative abundance of the class Burkholderiales (n = 48). Each dot represents measurements of a single mouse. The Spearman's rank correlation coefficient r and a linear regression line are shown. AU, arbitrary unit.

weights that reflect steatosis. Our data also confirm that the impairment of the intestinal barrier and body weight gain are 2 possible but likely independent consequences resulting from the diet. Although these findings derive from female mice only, the results are most likely not sex-specific because previous permeability studies have found no sex-dependent differences in mice (32). We have shown previously that the intake of glucose at high amounts induces a pronounced body weight gain and only minor liver weight gain, whereas fructose acts the other way around (16). In another set of experiments, we found that toll-like receptor-4 knockout mice are protected from fructose-induced liver steatosis, indicating that translocated endotoxin is a major trigger for fructose-induced liver steatosis (36). We subsequently studied not only the effects of sugars but also those of the WSD combining a high load of fat and sugar (17). The data herein reveal that a WSD, leading to a higher energy intake, resulted in a pronounced weight gain but only weak liver weight gain, whereas a WSD combined with a high fructose load promoted body weight gain and higher liver weight. This effect on the liver was even more pronounced than what was induced by fructose alone. The addition of fructose solution to the CD was not associated with a higher energy intake but caused increased liver weight, whereas body weight remained unchanged. These observations strongly suggest that increased energy intake causes body weight gain, as indicated by the close correlation we found between the 2 parameters, whereas high fructose intake has metabolic consequences because of as yet unknown mechanisms that might be related to barrier impairment and endotoxin translocation. These observations may have major implications for human disease because liver steatosis is an early indicator of insulin resistance and other metabolic complications occurring in obese individuals (38).

We found that all 4 experimental diets in our study caused a marked change in the overall microbiota composition, as revealed by the nonmetric multidimensional scaling of the data and analysis of the α diversity that decreased in all 4 diet groups. The likely reason behind this is that the experimental diets (CD and WSD) compared with the SD-B administered before the beginning of the study contained a rather high portion of carbohydrates, namely sucrose, but also a slightly higher quantity of fibers, which are both known to affect intestinal microbiota (39, 40). A WSD is defined as a sugar- and fat-rich diet, and the CD had a similar composition to the WSD except for a lower fat content. Fructose is a substrate for selected intestinal bacteria, as shown by stable isotope probing, and thus might modulate the microbiota by promoting the selective growth of particular commensals (41). The first evidence that fructose affects the microbiota comes from a few recent studies in rats that showed that orally administered fructose enhances the abundance of Enterobacteriaceae, *Coprococcus*, and *Ruminococcus* and induces a distinct fecal metabolome profile that is associated with fructose-induced nonalcoholic fatty liver disease (42, 43). We were also able to show that fructose increased the Firmicutes:Bacteroidetes ratio by reducing the abundance of Bacteroidetes phyla. Our data confirm the finding of Goodrich et al. (44), who reported that environmental factors, such as diet, affect Bacteroidetes more than Firmicutes, which are largely regulated by the genetic makeup of the host. Previous studies

have reported that high-fat diets increase this ratio (45, 46). However, in our study, we did not find an effect on the Firmicutes:Bacteroidetes ratio of WSD treatment (compared with CD), whereas fructose induced a clearly significant increase in both the CD + fructose and WSD + fructose groups compared with the CD group. It has recently been shown that the family of Peptostreptococcaceae increased in mice fed a high-calorie diet that led to nonalcoholic fatty liver disease (47). In our experiments, we found that the change from a low-sucrose SD-B to a high-sucrose CD causes a pronounced increase in Peptostreptococcaceae abundance. These data suggest that this genus is a consistent marker of an unhealthy high-sugar and energy-dense diet.

Most interestingly, we observed a sharp increase in the relative abundance of the *Bifidobacterium* genus in mice fed a WSD combined with a fructose challenge. These results are different from previous studies that have shown that a high-fat diet disrupts the intestinal microbiota by 2 means: first by diminishing the abundance of gut barrier–protecting Bifidobacteria and second by promoting the growth of endotoxin producers (48). In our experiments, we found an impaired barrier in the WSD + fructose group of mice, as assessed by endotoxin translocation, mucus loss, and other parameters, although Bifidobacteria were more abundant in this group than in the CD group. Bifidobacteria are known to use fructo-oligosaccharides, fructose, and sucrose as a substrate (49), whereas a WDS might promote small-intestine bowel overgrowth. The combination of a WSD and fructose could thus lead to a rise in Bifidobacteria, either directly or as a consequence of the bacterial overgrowth in the small intestine induced by fructose. Specific analyses of the microbiota in this part of the gut would be required to support this hypothesis.

Our study also revealed that a WSD causes an increase in gram-negative Burkholderiales and that this β-Proteobacteria order correlates with body weight gain. This confirms data from humans that have shown a correlation between specific Burkholderiales and weight gain in psychiatric patients (50). We found that the change from a lower-sugar SD-B to a high-sugar CD decreased Burkholderiales abundance, suggesting that components of the fat fraction rather than the sugars within the WSD are responsible for the increase (compared with SD-B) of these bacteria. Unfortunately, endotoxin or mucus and TJ measurements that require killing the mice could not be performed at the beginning of the study. Therefore, we could not determine to what extent changes in Burkholderiales are associated with gut barrier impairments.

The clinical impact of the reduction of *Parabacteroides* in mice fed a WSD is unclear at present. Previous studies have reported conflicting results for different *Parabacteroides* species: *P. allisonella* and *P. distasonis* have been shown to be increased in nonalcoholic steatohepatitis and obese patients, respectively (51, 52). *Barnesiella*, a Bacteroidetes from the Porphyromonadaceae family, was less abundant in mice fed a WSD, confirming data from Liu et al. (53) that showed that a high-fat diet reduces Porphyromonadaceae abundance in mice. This might have health consequences because *Barnesiella* and the bacterial family to which it belongs promote resistance to the colonization of different pathogens in the intestine (54).

In conclusion, our data indicate that a WSD, liquid fructose, and possibly a sucrose-rich diet affect the intestinal microbiome and barrier in different ways. This might explain why a WSD and sucrose primarily promote weight gain, whereas fructose, especially when combined with a WSD, results in pronounced gut barrier dysfunction.

Acknowledgments

We thank Andreas Rings for excellent technical support. VV and SCB designed the research; VV, SL, DP, LL, and MJO conducted the experiments and analyzed the data; MJO and JW provided essential reagents; SL and SCB wrote the manuscript; and SCB had primary responsibility for the final content. All authors read and approved the final manuscript.

References

1. Iggman D, Rosqvist F, Larsson A, Arnlöv J, Beckman L, Rudling M, Risérus U. Role of dietary fats in modulating cardiometabolic risk during moderate weight gain: a randomized double-blind overfeeding trial (LIPOGAIN study). J Am Heart Assoc 2014;3:e001095.
2. Johannsen DL, Tchoukalova Y, Tam CS, Covington JD, Xie W, Schwarz JM, Bajpeyi S, Ravussin E. Effect of 8 weeks of overfeeding on ectopic fat deposition and insulin sensitivity: testing the "adipose tissue expandability" hypothesis. Diabetes Care 2014;37:2789–97.
3. Giles ED, Wellberg EA, Astling DP, Anderson SM, Thor AD, Jindal S, Tan AC, Schedin PS, Maclean PS. Obesity and overfeeding affecting both tumor and systemic metabolism activates the progesterone receptor to contribute to postmenopausal breast cancer. Cancer Res 2012;72:6490–501.
4. Marwitz SE, Woodie LN, Blythe SN. Western-style diet induces insulin insensitivity and hyperactivity in adolescent male rats. Physiol Behav 2015;151:147–54.
5. Sample CH, Martin AA, Jones S, Hargrave SL, Davidson TL. Western-style diet impairs stimulus control by food deprivation state cues: implications for obesogenic environments. Appetite 2015;93:13–23.
6. Newmark HL, Yang K, Kurihara N, Fan K, Augenlicht LH, Lipkin M. Western-style diet-induced colonic tumors and their modulation by calcium and vitamin D in C57Bl/6 mice: a preclinical model for human sporadic colon cancer. Carcinogenesis 2009;30:88–92.
7. De Filippo C, Cavalieri D, Di Paola M, Ramazzotti M, Poullet JB, Massart S, Collini S, Pieraccini G, Lionetti P. Impact of diet in shaping gut microbiota revealed by a comparative study in children from Europe and rural Africa. Proc Natl Acad Sci USA 2010;107:14691–6.
8. Wu GD, Chen J, Hoffmann C, Bittinger K, Chen YY, Keilbaugh SA, Bewtra M, Knights D, Walters WA, Knight R, et al. Linking long-term dietary patterns with gut microbial enterotypes. Science 2011;334:105–8.
9. David LA, Maurice CF, Carmody RN, Gootenberg DB, Button JE, Wolfe BE, Ling AV, Devlin AS, Varma Y, Fischbach MA, et al. Diet rapidly and reproducibly alters the human gut microbiome. Nature 2014;505:559–63.
10. Turnbaugh PJ, Ley RE, Mahowald MA, Magrini V, Mardis ER, Gordon JI. An obesity-associated gut microbiome with increased capacity for energy harvest. Nature 2006;444:1027–31.
11. Schulz MD, Atay C, Heringer J, Romrig FK, Schwitalla S, Aydin B, Ziegler PK, Varga J, Reindl W, Pommerenke C, et al. High-fat-diet-mediated dysbiosis promotes intestinal carcinogenesis independently of obesity. Nature 2014;514:508–12.
12. Lukens JR, Gurung P, Vogel P, Johnson GR, Carter RA, McGoldrick DJ, Bandi SR, Calabrese CR, Vande Walle L, Lamkanfi M, et al. Dietary modulation of the microbiome affects autoinflammatory disease. Nature 2014;516:246–9.
13. Claesson MJ, Jeffery IB, Conde S, Power SE, O'Connor EM, Cusack S, Harris HM, Coakley M, Lakshminarayanan B, O'Sullivan O, et al. Gut microbiota composition correlates with diet and health in the elderly. Nature 2012;488:178–84.
14. Ritze Y, Bárdos G, Claus A, Ehrmann V, Bergheim I, Schwiertz A, Bischoff SC. Lactobacillus rhamnosus GG protects against non-alcoholic fatty liver disease in mice. PLoS One 2014;9:e80169.
15. Nawrocki AR, Rodriguez CG, Toolan DM, Price O, Henry M, Forrest G, Szeto D, Keohane CA, Pan Y, Smith KM, et al. Genetic deletion and pharmacological inhibition of phosphodiesterase 10A protects mice from diet-induced obesity and insulin resistance. Diabetes 2014;63:300–11.
16. Bergheim I, Weber S, Vos M, Krämer S, Volynets V, Kaserouni S, McClain CJ, Bischoff SC. Antibiotics protect against fructose-induced hepatic lipid accumulation in mice: role of endotoxin. J Hepatol 2008;48:983–92.

17. Reichold A, Brenner SA, Spruss A, Förster-Fromme K, Bergheim I, Bischoff SC. Bifidobacterium adolescentis protects from the development of nonalcoholic steatohepatitis in a mouse model. J Nutr Biochem 2014;25:118–25.
18. Amann RI, Binder BJ, Olson RJ, Chisholm SW, Devereux R, Stahl DA. Combination of 16S rRNA-targeted oligonucleotide probes with flow cytometry for analyzing mixed microbial populations. Appl Environ Microbiol 1990;56:1919–25.
19. Johansson ME, Hansson GC. Preservation of mucus in histological sections, immunostaining of mucins in fixed tissue, and localization of bacteria with FISH. Methods Mol Biol 2012;842:229–35.
20. Volynets V, Rings A, Bárdos G, Ostaff MJ, Wehkamp J, Bischoff SC. Intestinal barrier analysis by assessment of mucus, tight junctions and alpha-defensins in healthy C57BL/6J and Balb/cJ mice. Tissue Barriers 2016;4:e1208468.
21. Wehkamp J, Wang G, Kubler I, Nuding S, Gregorieff A, Schnabel A, Kays RJ, Fellermann K, Burk O, Schwab M, et al. The Paneth cell alpha-defensin deficiency of ileal Crohn's disease is linked to Wnt/Tcf-4. J Immunol 2007;179:3109–18.
22. Wesolowska-Andersen A, Bahl MI, Carvalho V, Kristiansen K, Sicheritz-Pontén T, Gupta R, Licht TR. Choice of bacterial DNA extraction method from fecal material influences community structure as evaluated by metagenomic analysis. Microbiome 2014;2:19.
23. Schmieder R, Edwards R. Quality control and preprocessing of metagenomic datasets. Bioinformatics 2011;27:863–4.
24. Magoč T, Salzberg S. FLASH: fast length adjustment of short reads to improve genome assemblies. Bioinformatics 2011;27:2957–63.
25. University of Tübingen. MALT (MEGAN alignment tool) [Internet]. [cited 2015 Jun 3]. Available from: http://ab.inf.uni-tuebingen.de/software/malt.
26. University of Tübingen. MEGAN6 [Internet]. [cited 2015 Jun 20]. Available from: http://ab.inf.uni-tuebingen.de/software/megan6/download/welcome.html.
27. Mitra S, Förster-Fromme K, Damms-Machado A, Scheurenbrand T, Biskup S, Huson DH, Bischoff SC. Analysis of the intestinal microbiota using SOLiD 16S rRNA gene sequencing and SOLiD shotgun sequencing. BMC Genomics 2013;14(Suppl 5):S16.
28. Rinttilä T, Kassinen A, Malinen E, Krogius L, Palva A. Development of an extensive set of 16S rDNA-targeted primers for quantification of pathogenic and indigenous bacteria in faecal samples by real-time PCR. J Appl Microbiol 2004;97:1166–77.
29. Bacchetti De Gregoris T, Aldred N, Clare AS, Burgess JG. Improvement of phylum- and class-specific primers for real-time PCR quantification of bacterial taxa. J Microbiol Methods 2011;86:351–6.
30. Matsuki T, Watanabe K, Fujimoto J, Kado Y, Takada T, Matsumoto K, Tanaka R. Quantitative PCR with 16S rRNA-gene-targeted species-specific primers for analysis of human intestinal bifidobacteria. Appl Environ Microbiol 2004;70:167–73.
31. Quast C, Pruesse E, Yilmaz P, Gerken J, Schweer T, Yarza P, Peplies J, Glöckner FO. The SILVA ribosomal RNA gene database project: improved data processing and web-based tools. Nucleic Acids Res 2013;41 D1:D590–6.
32. Volynets V, Reichold A, Bárdos G, Rings A, Bleich A, Bischoff SC. Assessment of the intestinal barrier with five different permeability tests in healthy C57BL/6J and BALB/cJ mice. Dig Dis Sci 2016;61:737–46.
33. R Foundation for Statistical Computing. R: a language and environment for statistical computing [Internet]. [cited 2015 Aug 3]. Available from: http://www.R-project.org.
34. Venables WN, Ripley BD. Modern applied statistics with S. 4th ed. New York: Springer; 2002.
35. Oksanen FJ, Blanchet FG, Kindt R, Legendre P, Minchin PR, O'Hara RB, Simpson GL, Solymos PM, Stevens HH, Wagner H. Vegan: community ecology package. R package version 2.3-0 [Internet]. [cited 2015 Aug 3]. Available from: https://cran.r-project.org/src/contrib/Archive/vegan/.
36. Spruss A, Kanuri G, Wagnerberger S, Haub S, Bischoff SC, Bergheim I. Toll-like receptor 4 is involved in the development of fructose-induced hepatic steatosis in mice. Hepatology 2009;50:1094–104.
37. Günzel D, Yu AS. Claudins and the modulation of tight junction permeability. Physiol Rev 2013;93:525–69.
38. Cusi K. Role of obesity and lipotoxicity in the development of nonalcoholic steatohepatitis: pathophysiology and clinical implications. Gastroenterology 2012;142:711–25.e6.
39. Parks BW, Nam E, Org E, Kostem E, Norheim F, Hui ST, Pan C, Civelek M, Rau CD, Bennett BJ, et al. Genetic control of obesity and gut microbiota composition in response to high-fat, high-sucrose diet in mice. Cell Metab 2013;17:141–52.
40. Simpson HL, Campbell BJ. Review article: dietary fibre-microbiota interactions. Aliment Pharmacol Ther 2015;42:158–79.
41. Michinaka A, Fujii T. Efficient and direct identification of fructose fermenting and non-fermenting bacteria from calf gut microbiota using stable isotope probing and modified T-RFLP. J Gen Appl Microbiol 2012;58:297–307.
42. Jena PK, Singh S, Prajapati B, Nareshkumar G, Mehta T, Seshadri S. Impact of targeted specific antibiotic delivery for gut microbiota modulation on high-fructose-fed rats. Appl Biochem Biotechnol 2014;172:3810–26.
43. Di Luccia B, Crescenzo R, Mazzoli A, Cigliano L, Venditti P, Walser JC, Widmer A, Baccigalupi L, Ricca E, Iossa S. Rescue of fructose-induced metabolic syndrome by antibiotics or faecal transplantation in a rat model of obesity. PLoS One 2015;10:e0134893.
44. Goodrich JK, Waters JL, Poole AC, Sutter JL, Koren O, Blekhman R, Beaumont M, Van Treuren W, Knight R, Bell JT, et al. Human genetics shape the gut microbiome. Cell 2014;159:789–99.
45. Turnbaugh PJ, Ridaura VK, Faith JJ, Rey FE, Knight R, Gordon JI. The effect of diet on the human gut microbiome: a metagenomic analysis in humanized gnotobiotic mice. Sci Transl Med 2009;1:6ra14.
46. Hildebrandt MA, Hoffmann C, Sherrill-Mix SA, Keilbaugh SA, Hamady M, Chen YY, Knight R, Ahima RS, Bushman F, Wu GD. High-fat diet determines the composition of the murine gut microbiome independently of obesity. Gastroenterology 2009;137:1716–24.e1–2.
47. Matsushita N, Osaka T, Haruta I, Ueshiba H, Yanagisawa N, Omori-Miyake M, Hashimoto E, Shibata N, Tokushige K, Saito K, et al. Effect of lipopolysaccharide on the progression of non-alcoholic fatty liver disease in high caloric diet-fed mice. Scand J Immunol 2016;83:109–18.
48. Cani PD, Neyrinck AM, Fava F, Knauf C, Burcelin RG, Tuohy KM, Gibson GR, Delzenne NM. Selective increases of bifidobacteria in gut microflora improve high-fat-diet-induced diabetes in mice through a mechanism associated with endotoxaemia. Diabetologia 2007;50:2374–83.
49. Wang X, Gibson GR. Effects of the in vitro fermentation of oligofructose and inulin by bacteria growing in the human large intestine. J Appl Bacteriol 1993;75:373–80.
50. Bahr SM, Tyler BC, Wooldridge N, Butcher BD, Burns TL, Teesch LM, Oltman CL, Azcarate-Peril MA, Kirby JR, Calarge CA. Use of the second-generation antipsychotic, risperidone, and secondary weight gain are associated with an altered gut microbiota in children. Transl Psychiatry 2015;5:e652.
51. Wong VW, Tse CH, Lam TT, Wong GL, Chim AM, Chu WC, Yeung DK, Law PT, Kwan HS, Yu J, et al. Molecular characterization of the fecal microbiota in patients with nonalcoholic steatohepatitis—a longitudinal study. PLoS One 2013;8:e62885.
52. Haro C, Montes-Borrego M, Rangel-Zúñiga OA, Alcalá-Díaz JF, Gómez-Delgado F, Pérez-Martínez P, Delgado-Lista J, Quintana-Navarro GM, Tinahones FJ, Landa BB, et al. Two healthy diets modulate gut microbial community improving insulin sensitivity in a human obese population. J Clin Endocrinol Metab 2016;101:233–42.
53. Liu T, Hougen H, Vollmer AC, Hiebert SM. Gut bacteria profiles of Mus musculus at the phylum and family levels are influenced by saturation of dietary fatty acids. Anaerobe 2012;18:331–7.
54. Ubeda C, Bucci V, Caballero S, Djukovic A, Toussaint NC, Equinda M, Lipuma L, Ling L, Gobourne A, No D, et al. Intestinal microbiota containing Barnesiella species cures vancomycin-resistant Enterococcus faecium colonization. Infect Immun 2013;81:965–73.